1-1-2014

Switch from canonical to noncanonical Wnt signaling mediates high glucose-induced adipogenesis

Emily C. Keats
Schulich School of Medicine & Dentistry

James M. Dominguez
University of Florida

Maria B. Grant
University of Florida

Zia A. Khan
Schulich School of Medicine & Dentistry, zia.khan@schulich.uwo.ca

STEM CELLS®

TISSUE-SPECIFIC STEM CELLS

Switch from Canonical to Noncanonical Wnt Signaling Mediates High Glucose-Induced Adipogenesis

EMILY C. KEATS,[a] JAMES M. DOMINGUEZ II,[b] MARIA B. GRANT,[b,d] ZIA A. KHAN[a,c]

Key Words. Adipogenesis • Diabetes • Wnt signaling • Protein kinase C • Noncanonical signaling • Cell-autogenous regulation

[a]Department of Pathology, Schulich School of Medicine & Dentistry, University of Western Ontario, London, Ontario, Canada; [b]Department of Pharmacology and Therapeutics, College of Medicine, University of Florida, Gainesville, Florida, USA; [c]Metabolism and Diabetes Program, Lawson Health Research Institute, London, Ontario, Canada; [d]Department of Ophthalmology, Indiana University School of Medicine, Indianapolis, Indiana

Correspondence: Zia A. Khan, Ph.D., 4011 Dental Sciences Building, 1151 Richmond Street, London, Ontario, Canada N6A 5C1. Telephone: 519-661-2111, ext. 81562; Fax: 519-661-3370; e-mail: zia.khan@schulich.uwo.ca

Received October 6, 2013; accepted for publication January 11, 2014; first published online in STEM CELLS *EXPRESS* February 4, 2014.

1066-5099/2014/$30.00/0

http://dx.doi.org/10.1002/stem.1659

ABSTRACT

Human bone marrow mesenchymal progenitor cells (MPCs) are multipotent cells that play an essential role in endogenous repair and the maintenance of the stem cell niche. We have recently shown that high levels of glucose, conditions mimicking diabetes, cause impairment of MPCs, resulting in enhanced adipogenesis and suppression of osteogenesis. This implies that diabetes may lead to reduced endogenous repair mechanisms through altering the differentiation potential of MPCs and, consequently, disrupting the stem cell niche. Phenotypic alterations in the bone marrow of long-term diabetic patients closely resemble this observation. Here, we show that high levels of glucose selectively enhance autogenous Wnt11 expression in MPCs to stimulate adipogenesis through the Wnt/protein kinase C noncanonical pathway. This novel mechanism may account for increased bone marrow adipogenesis, severe bone loss, and reduced vascular stem cells leading to chronic secondary complications of diabetes. STEM CELLS *2014;32:1649–1660*

INTRODUCTION

Human bone marrow mesenchymal progenitor cells (MPCs; also known as mesenchymal stem cells, marrow stromal cells, and multipotent adult progenitor cells) are a pool of multipotent cells that give rise to adipocytes, osteoblasts, chondrocytes, and perivascular cells. Although direct associations between MPC dysfunction and diabetes have been elusive, the deregulation of MPC progeny is a likely outcome of the chronic metabolic perturbations seen in diabetes. Diabetes has been associated with fatty bone marrow [1, 2], alongside moderate to severe bone loss [3–5] and increased fracture risk [6, 7]. Diabetes also induces microvascular remodeling in the bone marrow [8, 9] manifesting as impaired angiogenic ability, endothelial cell dysfunction, increased oxidative stress, and a reduction in stem cell number [8]. Taken together, it would appear that disruption of the bone marrow microenvironment in diabetes might have detrimental consequences on stem/progenitor cell function and differentiation.

We have previously demonstrated that high levels of glucose, similar to levels seen in diabetes, cause dysfunction of MPCs [10]. MPCs showed skewed differentiation toward the adipocyte lineage, while their ability to become osteoblasts and chondrocytes was impaired. This is the first indication of glucose levels regulating MPC fate determination. Not only does this alteration provide an important link between diabetes and obesity, but it may also account for the long-term changes that are occurring in diabetic marrow. The mechanisms underlying this association, however, remain undiscovered. These mechanisms may involve Wingless-type mouse mammary tumor virus integration site family members (Wnts), a family of secreted glycoproteins that play a role in cell fate determination and development [11]. In some of the early work implicating Wnt signaling in adipogenesis, Ross et al. showed that preadipocytes can be maintained in an undifferentiated state using Wnt10b, which was later shown to be mediated by blocking peroxisome proliferator-activated receptor γ (PPARγ) and CCAAT-enhancer-binding protein α (C/EBPα) [12]. These, and other, findings led to the notion that Wnt signaling acts as a switch during adipogenesis; when switched off, differentiation of committed preadipocytes is able to proceed. To date however, the role of Wnt signaling, canonical or noncanonical (i.e., β-catenin-dependent and -independent, respectively), in human MPC lineage commitment has been controversial. Previous studies have shown that high glucose

(HG) levels cause Wnt activation and nuclear β-catenin accumulation in a number of human cancer cell lines [13], macrophages [14], and mesangial cells [15]. Therefore, it is crucial to understand how MPC differentiation is regulated and to decipher the role of Wnt signaling in this process.

In this study, we systematically investigate the molecular mechanisms that are responsible for the HG-mediated alterations in MPC differentiation. We hypothesize that HG is enhancing adipogenesis through selective modulation of Wnt signaling, and that this mechanism is directly responsible for the long-term phenotypic changes that are seen in the diabetic bone marrow.

Materials and Methods

Isolation and Culture of MPCs

All experiments were approved by the Research Ethics Board at the University of Western Ontario, London, Ontario, Canada. Fresh bone marrow samples (1M-125, Lonza, Inc., Walkersville, MD, www.lonza.com) were obtained and mononuclear cell fraction was prepared as shown by us previously [10, 16]. Bone marrow samples were cultured on fibronectin-coated (FN; 1 $\mu g/cm^2$; FC010-10MG, Millipore, Temecula, CA, www.millipore.com) plates in Dulbecco's modified Eagle's medium (DMEM) low glucose with pyruvate and L-glutamine (10–014-CV, Mediatech, Manassas, VA, www.cellgro.com) media, supplemented with 20% fetal bovine serum (FBS; Life Technologies, Burlington, Canada, www.lifetechnologies.com), 1× penicillin-streptomycin-amphotericin (PSF; Mediatech), and no additional growth factors. We have shown that in the presence of serum, bone marrow cells lose the ability to produce clonal populations and differentiate into endothelial cells and neuroglial cells [17]. Therefore, we refer to these cells as MPCs as they retain the ability to produce mesenchymal lineages: adipocytes, chondrocytes, and osteoblasts [10, 18]. All experiments using bone marrow-derived MPCs (bmMPCs) were conducted on passage 2–6 cells with at least three technical and three to five biological replicates.

To induce differentiation, we seeded MPCs at 40,000 cells per square centimeter on 12-well or 24-well plates in specific differentiation media but without FN coating (StemPro Adipogenesis; Life Technologies). The components of the STEMpro media are proprietary. However, it does not contain any PPARγ agonists and we are able to reproduce our results with DMEM/10% FBS, 5 μg/ml insulin, 1 μM dexamethasone (D2915; Sigma-Aldrich, Oakville, Canada, www.sigmaaldrich.com), 0.5 mM isobutylmethylxanthine (I7018; Sigma-Aldrich), 60 μM indomethacin (I7378; Sigma-Aldrich), and 1× PSF. However, for the ease of use and low intra-assay variability, we used StemPro for our studies. We also plated cells at high density to study mechanisms specifically at play during differentiation without the confounding effect of early proliferation, which takes place in most differentiation assays. Control or differentiation media were supplemented with HG (25 mmol/l final concentration). Control media formulation contains approximately 5.5 mM glucose (100 mg/dl), which approximates to normal blood glucose levels in vivo. In cell culture studies, concentrations of glucose approaching 10 mM (180 mg/dl) are considered prediabetic and concentrations above 10 mM are analogous to diabetic condition. To study the effect of HG, conditions mimicking diabetes, we have used 25 mM glucose levels (450 mg/dl). We also tested the effect of recombinant Wnt5a (50 ng/ml; 645-WN-010, R&D Systems, Minneapolis, MN, www.rndsystems.com), Wnt5b (50 ng/ml; 7347-WN-025, R&D Systems), and Wnt11 (50 ng/ml; 6179-WN-010, R&D Systems) in adipogenic differentiation media. IWR-1-endo (13659-10, Cayman Chemical, Ann Arbor, MI, www.caymanchem.com) and PNU74654 (3534/10, R&D Systems), both were added at concentrations of 5, 10, and 20 μM. A Wnt signaling agonist (Calbiochem CAS 853220-52-7; Millipore) was also used and added at concentrations varying from 100 nM to 5 μM. In Solution Rac1 Inhibitor II Z62954982 (25 μM, 553512; Millipore), Rho Kinase Inhibitor VII (10 nM; 555556; EMD Millipore), pan-protein kinase C (PKC) inhibitor chelerythrine chloride (700 nM, 1278; Cayman Chemicals), specific epsilon-PKC Inhibitor (5 μM; 62187 [AN]; Anaspec, Inc., Fremont, CA, www.anaspec.com), and calmodulin-dependent kinase inhibitor KN93 (500 nM, 1278; Tocris Biosciences; Bristol, U.K., www.tocris.com) were also used depending on the experiment. Media were changed every other day. RNA was isolated from cells in order to perform qRT-PCR. For oil red O staining, cells were fixed in 10% neutral buffered formalin and placed in 100% propylene for 5 minutes before applying 0.5% oil red O solution (O0625-25G, Sigma-Aldrich).

RNA Isolation and qRT-PCR

Using RNeasy Mini Plus or Micro Plus (Qiagen, Mississauga, Canada, www.qiagen.com), total RNA was extracted from the cells grown in culture. The quantity was determined by Qubit Broad Range RNA assay in the Qubit Fluorometer (Life Technologies). cDNA synthesis was performed with iScript cDNA Synthesis Kit (Bio-Rad Laboratories, Hercules, CA, www.bio-rad.com). To examine the human Wnt signaling pathway, a 96-well RT^2 Profiler PCR Array (Qiagen; PAHS-043Z) was used with RT^2 SYBR Green Mastermix (Qiagen) to profile the expression of 84 genes. Data were analyzed by CFX Manager Software using $\Delta\Delta$CT method with β-actin normalization and reported as relative expression. For all other mRNA analyses, reactions consisted of 10 μl SsoFast EvaGreen Supermix (Bio-Rad), 2 μl of both forward and reverse primers (at 10 μM concentration), 1 μl cDNA, and 6 μl of H_2O. All primer sets were predesigned and obtained from Qiagen except for PPARγ2 (sequence [10]). All reactions were performed for 40 cycles using the following temperature profiles: 95°C for 2 minutes (initial denaturation); and 55°C for 12 seconds (annealing and extension). Data were analyzed using $\Delta\Delta$CT method with β-actin normalization and reported as relative expression.

Human Bone Marrow Samples

We obtained paraffin and frozen human femoral bone marrow tissue slides of both control (U.S. Biomax, Rockville, MD, $n = 3$; age 63 ± 2.64 years) and type 2 diabetic patients (U.S. Biologicals, Salem, MA; U.S. Biomax, and BioChain Institute, Hayward, CA; $n = 4$, age 65.33 ± 2.33 years/body mass index and duration of diabetes unknown). cDNA samples from control and type 2 diabetic patients were obtained from BioChain Institute. Studies were approved by the Research Ethics Board at the University of Western Ontario, Canada. Double staining was performed using Picture Plus Double Staining Kit (Life Technologies). Slides were deparaffinized, hydrated through a sequential ethanol gradient, and washed in PBS. Slides were then subjected to antigen retrieval in Tris-EDTA buffer (10 mM Trizma-base, 1 mM EDTA,

0.05% Tween-20, pH 9.0) and 120°C for 20 minutes using the Antigen Retriever (2100 Retriever, PickCell Laboratories, Electron Micrscopy Sciences, Hatfield, PA, www.emsdiasum.com). Following antigen retrieval, endogenous peroxidase activity was quenched with 3% H_2O_2 diluted in methanol for 10 minutes. Slides were blocked and primary antibodies (CD133 antibody, ab19898, Abcam, Cambridge, MA, www.abcam.com; CD45 antibody, MAB1430, R&D Systems) were applied simultaneously for 1 hour. Slides were rinsed in phosphate-buffered saline (PBS) containing 0.05% Tween-20. Goat anti-mouse IgG-horseradish peroxidase polymer conjugate and goat anti-rabbit IgG-alkaline phosphatase polymer conjugate were then applied for 30 minutes. Diaminobenzidine (DAB) chromogen and Fast Red were used for detection. Slides were counterstained with Mayer's hematoxylin (Sigma-Aldrich) for 30 seconds and mounted using ClearMount Mounting solution (Life Technologies). Images were taken using Olympus BX-51 microscope (Olympus Canada, Inc., Richmond Hill, Canada, www.olympuscanada.com) equipped with a Spot Pursuit digital camera (SPOT Imaging Solutions, www.spotimaging.com, Sterling Heights, MI).

Diabetic Animal Model

Streptozotocin-induced diabetic rat model was used. A single intraperitoneal injection of freshly prepared streptozotocin (65 mg/kg in citrate buffer, pH 4.5) was performed in 8-week-old Sprague-Dawley rats (Harlan Laboratories, Indianapolis, IN, www.harlan.com). Diabetes was confirmed after 1 week following streptozotocin injection by measuring the blood glucose level (>200 mg/dl; >11 mmol/l) using the FreeStyle glucomonitor (www.myfreestyle.com). Following 2 months of diabetes, rats were euthanized and femoral bones were removed, decalcified, and embedded in paraffin. Tissues were sectioned at 5 μm. All animal procedures were in compliance with the National Institutes of Health Guide for the Care and Use of Laboratory Animals. The protocols for the rat studies were approved by the Institutional Animal Care and Use Committee at the University of Florida.

Rat bone marrow slides were deparaffinized, hydrated, and subjected to antigen retrieval as outlined above. Primary antibodies (Wnt11, ab96730, Abcam; Angiopoietin 2, ab153934, Abcam) were applied for 1 hour. Alexa488-conjugated secondary antibody (Life Technologies) was used for detection. Slides were counterstained with 4′,6-diamidino-2-phenylindole (DAPI) (Vector Laboratories) and mounted using Fluoromount K 024 (Diagnostic BioSystems, Pleasanton, CA, www.dbiosys.com). Fluorescence images were taken using Olympus BX-51 microscope and contrast images were taken with Fluoview FV10i Confocal Laser Scanning Biological Microscope (Olympus).

Cell Transfections

MPCs were grown in culture in DMEM/20% FBS until confluent. On the day of transfection, cells were trypsinized and resuspended with control or β-catenin siRNA (30 nM final concentration; Santa Cruz Biotechnologies, Santa Cruz, CA, www.scbt.com, sc-29209) and subjected to electroporation (1,400 V, 20 ms, 2 pulses) using Neon Transfection System (Life Technologies). For simultaneous knockdown of Wnt11 and β-catenin, cells were trypsinized and resuspended in a mixture of both siRNA sets (30 nM each; Wnt11 siRNA sc-41120, Santa Cruz Biotechnologies) and transfected as before. Knockdown efficiency was determined at day 7 in normal growth media or adipogenesis media by real-time RT-PCR and enzyme-linked immunosorbent assay. GFP-RhoA Expression Vector Set (contains dominant negative and wild type; STA-452, Cell BioLabs, San Diego, CA, www.cellbiolabs.com) or GFP-Rac1 Expression Vector Set (contains dominant negative and wild type; STA-450, Cell BioLabs) were also used at 1 μg using the same electroporation protocol as for siRNA. Transfected cells were transferred to a 24-well plate containing DMEM media without antibiotics. The following day, the media were changed to adipogenic media (StemPro Adipogenesis Differentiation media) with or without the addition of HG.

PKC Activity Assay and Other Protein Measurements

Total protein was extracted using Cell Extraction Buffer (Life Technologies, FNN0011) with Halt Protease and Phosphatase Inhibitor Single-Use Cocktail (Thermo Scientific, Waltham, MA, www.thermofisher.com) to prevent enzymatic degradation. Total protein from each sample was then quantified using Pierce bicinchoninic acid (BCA) Protein Assay Kit (Thermo Scientific). Following quantification, total β-catenin (Life Technologies, KHO1211) and PKC kinase activity (Enzo Life Sciences, Farmingdale, NY, www.enzolifesciences.com, ADI-EKS-420A) were measured as per manufacturer's protocol. Data were normalized to μg total protein levels as determined by BCA. Angiopoietin-2 (Ang-2) and Wnt11 protein levels were measured by coating microtiter plates with cell culture media (0.05 M sodium carbonate-bicarbonate buffer; pH 9.6) for 2 hours. Recombinant human Ang2 (623-AN-025; R&D Systems) and Wnt11 in DMEM media were used to create standard curves. Plates were then blocked with PBS/1% bovine serum albumin for 2 hours. Rabbit anti-human Ang2 and Wnt11 antibodies were applied at 1:200 in blocking buffer for 1 hour. Anti-rabbit IgG-horseradish peroxidase was used for detection with 3,3′,5,5′-tetramethylbenzidine substrate. Data were normalized to μg total protein levels.

Cell Staining

Cultured cells were trypsinized and plated (15,000 cells per square centimeter) on FN-coated 8-chambered slides 1 day prior to staining to allow for attachment of cells. Immunofluorescence staining of MPCs for β-catenin (1:200, Abcam, ab6302) and phospho-PKC T497 (1:100; Abcam, ab59411) was carried out, followed by Alexa488-conjugated secondary antibody (Life Technologies). Images were taken using Olympus BX-51 microscope. β-Catenin staining intensity and localization were quantified by ImageJ analysis following background subtraction to account for slide to slide variability.

Statistical Analysis

The data were expressed as means ± SEM. Where appropriate, two-tailed Student's unpaired *t* tests or analysis of variance with Bonferroni correction were performed. *p* values < .05 were considered statistically significant.

Results

HG Primes MPCs to Alter Their Differentiation Potential

In our initial studies, we showed that exposure of MPCs to high levels of glucose (25 mmol/l; HG) enhances adipogenesis [10].

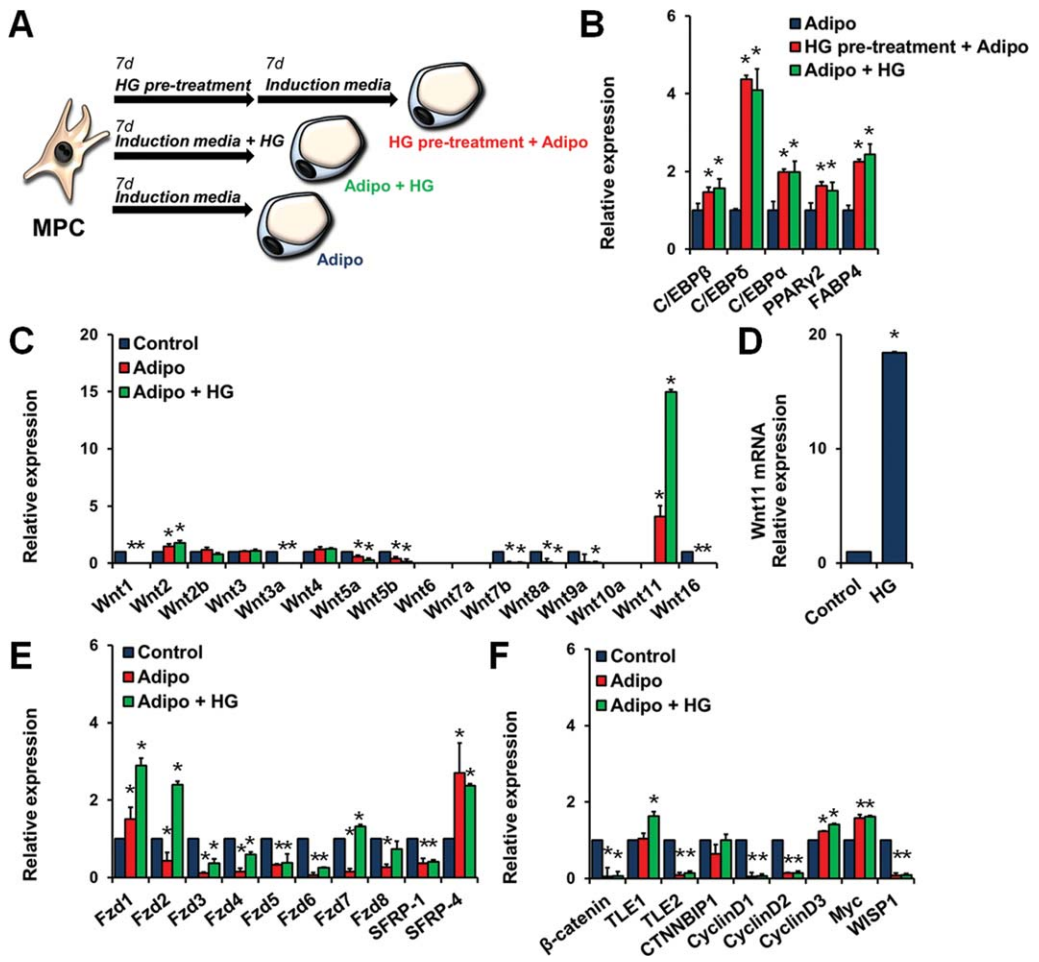

Figure 1. HG primes MPCs to alter their differentiation potential through selective modulation of Wnt signaling. **(A):** Schematic showing treatment groups for the HG priming study. **(B):** Extent of adipogenesis was measured by induction of adipogenesis-specific transcription factors: c/EBPβ and c/EBPδ (early transcription factors), c/EBPα and PPARγ2 (late transcription factors), and FABP4 (marker for differentiated adipocytes) (data are represented as mean $\pm$ SEM; *, $p < .05$ compared to adipogenic media [Adipo]). **(C):** MPCs were differentiated into adipocytes in the presence or absence of HG and mRNA expression of Wnt ligands was examined (data are represented as mean $\pm$ SEM; *, $p < .05$ compared to Control). **(D):** Wnt11 mRNA levels in MPCs after treatment with HG for 7 days in normal growth media (Dulbecco's modified Eagle's medium [DMEM]/10% FBS) (data are represented as mean $\pm$ SEM; *, $p < .05$ compared to Control [DMEM/10% media with 5 mmol/l glucose]). **(E):** mRNA levels of frizzled receptors and secreted frizzled-related proteins (SFRP-1 and -4) (data are represented as mean $\pm$ SEM; *, $p < .05$ compared to Control). **(F):** mRNA expression of β-catenin, negative transcriptional regulators of canonical Wnt signaling (TLE1/2; CTNNBIP1), and downstream target genes (CyclinD1/D2/D3; Myc; WISP1) in control, Adipo, and Adipo + HG groups (data are represented as mean $\pm$ SEM; *, $p < .05$ compared to Control). Abbreviations: Adipo, adipogenic induction media; CTNNBIP1, β-catenin interacting protein-1; HG, high glucose; MPC, mesenchymal progenitor cell; SFRP, secreted frizzled-related protein; TLE1/2, transducin-like enhancer proteins 1/2; WISP1, Wnt-induced secreted protein-1.

Therefore, we first wanted to assess whether the effect of HG on MPC differentiation was transient, or if HG reprogrammed the cells so that an increase in adipogenesis would still be evident with removal of the stimulus. To do this, we performed a "priming" study as shown in Figure 1A. We compared three experimental groups: (a) cells subjected to an adipogenesis assay only (Adipo), (b) cells pretreated with HG for 7 days in control media prior to the adipogenesis assay (HG pretreatment + Adipo), and (c) cells subjected to the adipogenesis assay in the presence of HG (Adipo + HG). Degree of adipogenesis, as noted by the induction level of adipogenesis-specific transcription factors c/EBPα/β/δ and PPARγ2, was similar in groups 2 and 3 (pretreatment group and Adipo + HG group), and was significantly higher than group 1 (Adipo alone; Fig. 1B). C/EBPβ and C/EBPδ play an important role in early adipocyte differentiation by inducing C/EBPα and PPARγ2. Higher levels of these adipogenesis-specific transcription factors following pretreatment of MPCs with HG suggest that glucose levels reprogram the differentiation capacity of MPCs. In further support, fatty acid binding protein-4 (FABP4; also known as adipocyte protein 2, aP2), which is a marker of fully differentiated adipocytes, was significantly higher in cells exposed to Adipo + HG media or with HG pretreatment alone (Fig. 1B). This again indicates that the effect of HG is not transitory.

HG Selectively Modulates Wnt Signaling During Adipogenesis

We used a real-time PCR-based array approach to profile the Wnt signaling pathway during the processes of adipogenesis in HG. Presence of HG in the induction media depressed the expression of most Wnt ligands (Fig. 1C). Interestingly, we saw a significant increase in autogenous Wnt11 expression by HG.

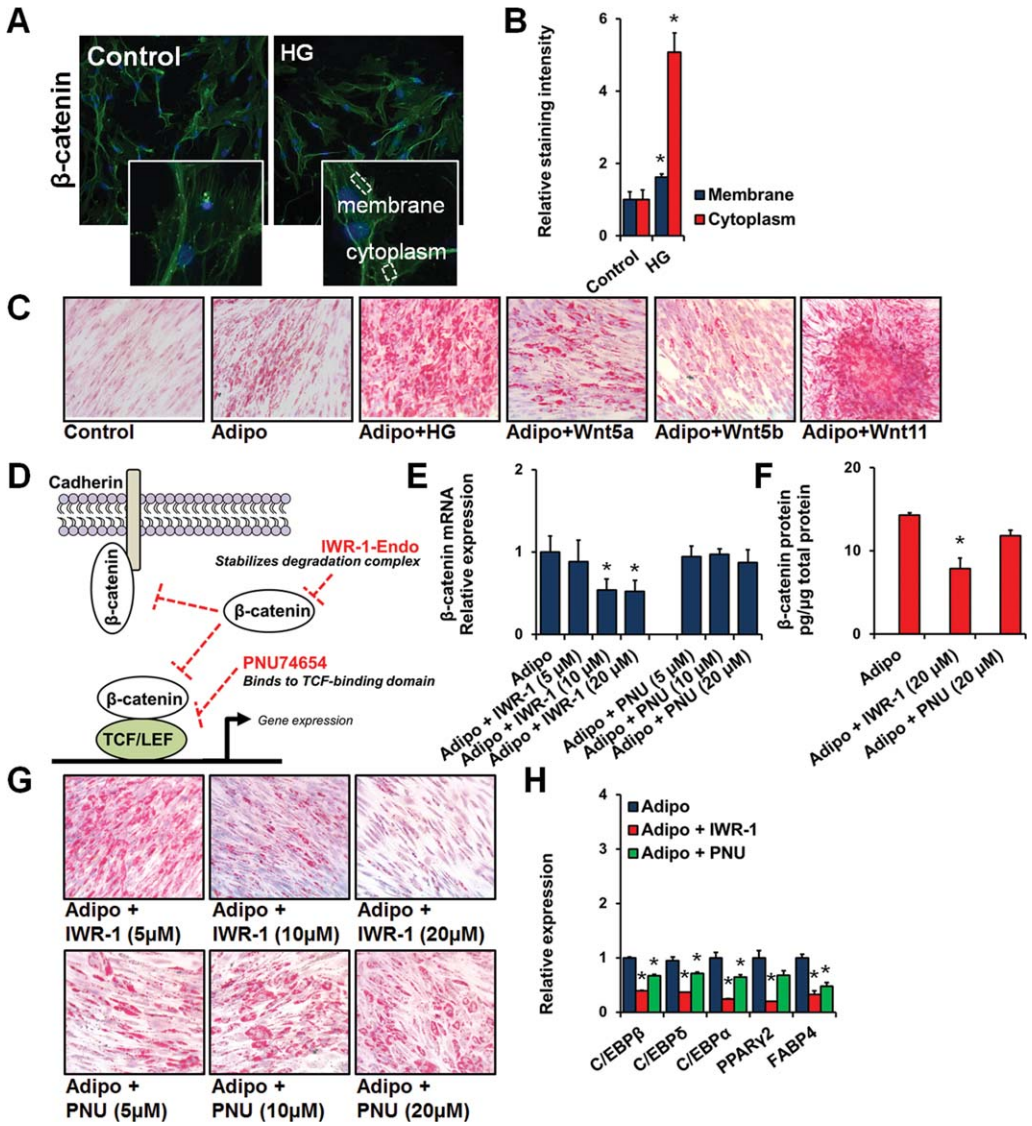

Figure 2. Small molecule inhibitors of the canonical Wnt pathway inhibit adipogenesis in mesenchymal progenitor cells (MPCs). **(A):** β-Catenin protein localization in MPCs after treatment with HG (25 mmol/l) for 24 hours in normal growth media (Green = β-catenin, blue = 4′,6-diamidino-2-phenylindole (DAPI); ×20 magnification; inset at ×40; highlighted areas in inset shows areas of focus for β-catenin localization). **(B):** Quantification of cytoplasmic and membrane β-catenin staining (data are represented as mean ± SEM; *, $p < .05$ compared to control). **(C):** Oil red O staining following adipogenesis showing MPCs in normal growth media (control) and cells exposed to Adipo (adipogenic induction media). HG and exogenous recombinant Wnt5a, Wnt5b, and Wnt11 (all at 50 ng/ml) were added to each assay separately (red color = lipid droplets). **(D):** Mechanism of action of the IWR-1-endo (IWR-1) and PNU74654 (PNU) Wnt signaling antagonists. **(E, F):** Effect of IWR-1 and PNU on β-catenin mRNA **(E)** and protein **(F)** levels (β-catenin protein levels normalized to total protein; data are represented as mean ± SEM; *, $p < .05$ as compared to Adipo). **(G):** Oil red O staining after the addition of IWR-1 and PNU at varying concentrations in Adipo media. **(H):** mRNA levels of adipogenesis-specific transcription factors and FABP4 after treatment with IWR-1 and PNU (data are represented as mean ± SEM; *, $p < .05$ compared to Adipo). Abbreviations: HG, high glucose; LEF, lymphoid enhancer-binding factor 1; TCF, T-cell factor.

Treatment of MPCs with HG alone (in normal/control media) also upregulated Wnt11 expression (Fig. 1D), indicating that HG specifically was responsible for this increase. In contrast to the Wnt ligands, frizzled receptors were also selectively modulated by HG (Fig. 1E). Analysis of β-catenin, β-catenin inhibitors (transducin-like enhancer proteins 1/2; β-catenin interacting protein-1, CTNNBIP1), and downstream target genes showed that HG does not induce β-catenin-mediated transcription (Fig. 1F). Most of the downstream target genes were significantly downregulated with the exception of Myc and cyclin D3. Interestingly, a recent study showed that inhibition of canonical β-catenin signaling (transcriptional mode) with downregulation of cyclin D1 but upregulated cyclin D3 is associated with myogenic differentiation in C2C12 mouse myoblast cell line [19]. Our results show a similar pattern of downregulation of cyclin D1/2 and upregulation of cyclin D3 with HG (Fig. 1F). We wanted to know whether HG is in fact, decreasing β-catenin-mediated transcription in MPCs and therefore, we treated MPCs with HG in normal media and assessed β-catenin localization. Both cytoplasmic and membrane β-catenin protein levels showed an increase (Fig. 2A, 2B), although it was absent from the nucleus illustrating that canonical Wnt signaling is not active. However, the intriguing behavior

of Wnt11 transcript levels in HG (with or without Adipo media) indicated a potential connection to noncanonical Wnt signaling.

Wnt11 Mediates the Effects of HG to Stimulate Adipogenesis

To determine whether Wnt11 mediates the effects of HG in enhancing adipogenesis, we performed MPC differentiation in the presence of exogenous Wnt proteins, and used oil red O staining to highlight resulting lipid droplets. Exogenous Wnt5a and Wnt5b, both downregulated by HG (Fig. 1C), showed no drastic effect on adipogenesis (Fig. 2C). However, with the addition of noncanonical Wnt11, the intensity of the oil red O staining increased mimicking the effects of HG. We further examined whether Wnt/β-catenin signaling was involved using small molecule inhibitors. IWR-1-endo (IWR-1) that inhibits canonical β-catenin-dependent signaling showed reduced adipogenesis with increasing concentrations (Fig. 2D–2H). Addition of IWR-1 also reduced mRNA levels of β-catenin (Fig. 2E) and slight but significant changes to the protein levels (Fig. 2F). This was expected as IWR-1 only degrades "free" β-catenin which is available to participate in the canonical Wnt pathway [20]. It should be noted that higher concentrations of IWR-1 (greater than 10 μM) were associated with noticeably reduced cell density possibly due to toxicity, which may influence MPC differentiation and our oil red O readout. PNU74654 (PNU), a blocker of β-catenin/T-cell factor/lymphoid enhancer factor interaction, showed no changes in oil red O staining, and mRNA and protein levels of β-catenin (Fig. 2D, 2G). However, mRNA levels of adipogenesis-specific transcription factors and FABP4 after PNU treatment revealed inhibition of C/EBPs and FABP4 but not PPARγ2 (Fig. 2H). We confirmed the role of β-catenin in adipogenesis using two further approaches. First, we treated MPCs with a Wnt agonist (a cell-permeable pyrimidine that increases intracellular β-catenin levels without altering the destruction complex) and observed enhanced adipogenesis (Fig. 3A). Then, we used siRNA to specifically knockdown the expression of β-catenin. Contrary to what we expected, a near complete knockdown of β-catenin dramatically increased adipogenesis (Fig. 3B–3D). These observations led us to hypothesize that there is a switch from canonical to noncanonical Wnt signaling upon β-catenin gene knockdown. Therefore, we examined the expression of the likely candidate, noncanonical Wnt11, in MPCs that were transfected with β-catenin siRNA and underwent adipogenesis. We noted drastically enhanced Wnt11 levels at the mRNA and protein levels (Fig. 3E, 3F) pointing to noncanonical signaling, and more specifically Wnt11 as the potential mediator of the HG-induced increase in adipogenesis. To provide experimental evidence for this switch, we simultaneously knocked down Wnt11 and β-catenin and subjected the cells to adipogenesis. Transfection of MPCs with β-catenin and Wnt11 siRNA led to a significant decrease in mRNA and protein levels of both factors (Fig. 3G–3I), and completely abolished adipogenesis that was seen with β-catenin depletion alone (Fig. 3J). This indicated that β-catenin depletion led to enhanced adipogenesis through induction of Wnt11.

Noncanonical Wnt Signaling Stimulates Adipogenesis

Our next objective was to dissect out the noncanonical Wnt pathway and determine whether Wnt/planar cell polarity (PCP) pathway or the Wnt/calcium (Ca^{2+}) pathway is involved in adipogenesis. To achieve this, we used genetic and chemical modulation of the key players in each segment of the noncanonical pathway. Important insights into PCP signaling emerged from studies in Drosophila, which uncovered an important role of Rho GTPases. Two members of the Rho family, RhoA and Rac1, play a central role in the Wnt/PCP pathway (reviewed in [21]). We transfected MPCs with dominant negative (DN) and wild-type (WT) Rac1 first. DN Rac1 enhanced adipogenesis as compared to WT transfected cells (Fig. 4A) suggesting that basal Rac1 activity may be inhibiting differentiation and dominant negative Rac1 may relieve this inhibition. Similar results were obtained when we inhibited Rac1 using a specific pharmacological Rac1 inhibitor (Z62954982; Fig. 4B). Furthermore, RhoA modulation by dominant negative transfection and Rho kinase Inhibitor VII confirmed that both Rac1 and RhoA have overlapping functions in MPCs (data not shown). Rac and Rho are believed to have opposing functions [22, 23]. This suggests that their role during adipogenesis may be related to cell shape change, which would result in overlapping readout.

Building on these studies, we examined the role of Wnt/Ca^{2+} pathway in adipogenesis. Inhibition of PKC through chelerythrine chloride (Che) or PCK-ε V1–2 [24], which specifically blocks the epsilon isoform of PKC, reduced adipogenesis in MPCs (Fig. 3C). To prevent signaling on the alternate side of the same pathway, we used KN93 to inhibit calcium/calmodulin-dependent kinase II (CAMKII). CAMKII paralleled PKC activity during MPC differentiation (Fig. 4C). These results demonstrate a positive role for the Wnt/Ca^{2+} pathway in the regulation of adipogenesis. Our previous results point to Wnt11 as mediating the effects of HG, therefore we tested whether Wnt11 would normalize the effects of PKC inhibition. Our hypothesis was that Wnt11 would decrease the level of PKC inhibition if it used the same pathway. We found that Wnt11 does significantly dampen the effects of both PKC inhibitors (Fig. 4C) suggesting that Wnt11 may mediate its effects by inducing PKC activity. We confirmed the role of PKC by measuring its activity and show that exogenous Wnt11 increases PKC activity in both Che and PKCε V1–2-treated cells (Fig. 4D). Next, we examined phospho-PKC (p-PKC) levels in human MPCs that had been treated with Wnt11 (50 ng/ml) for 24 hours in normal media. We found increased p-PKC in MPCs treated with Wnt11 (Fig. 4E). Increased p-PKC levels upon Wnt11 treatment were found to colocalize to the nucleus. This was an unusual and unexpected finding. Interestingly, PKCε has been shown to accumulate in the nuclei of 3T3-F442A cells [24].

Reduced CD133+ Stem Cells in Diabetic Bone Marrow

In order to investigate whether the enhanced differentiation of MPCs to adipocytes is a direct reflection of alterations occurring in the stem cell niche, we examined CD133-expressing cell number in human control and type 2 diabetic bone marrow samples. As human samples are quite difficult to procure, we were only able to obtain type 2 diabetic patient samples. However, this afforded us the ability to determine stem cell number unambiguously, as CD133 is specific to stem/progenitor cells in humans but not rodents. We used immunohistochemistry to stain for CD133+ cells that were devoid of CD45 reactivity and CD133+/CD45+ hematopoietic stem cells (HSCs). The rationale was to determine

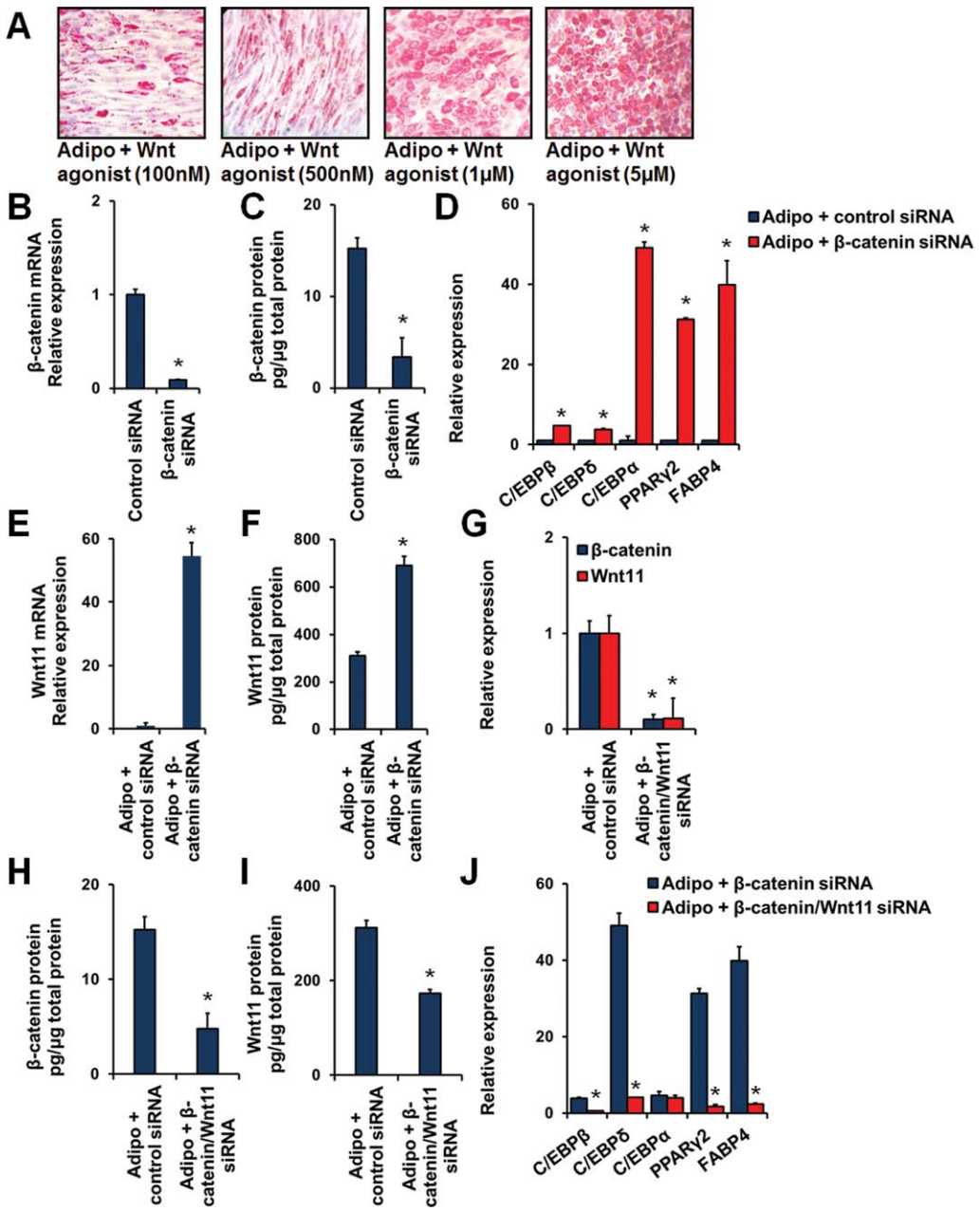

Figure 3. Depletion of β-catenin enhances adipogenesis in mesenchymal progenitor cells (MPCs) through induction of Wnt11. **(A):** Oil red O staining following exposure of MPCs to Wnt agonist for 7 days showed increased adipogenesis. **(B, C):** Levels of β-catenin mRNA **(B)** and protein **(C)** in MPCs 7 days after transfection with β-catenin siRNA (cells cultured in growth media following transfection; β-catenin protein levels normalized to total protein; data are represented as mean $\pm$ SEM; *, $p < .05$ compared to control siRNA). **(D):** Extent of adipogenesis after β-catenin siRNA transfection (data are represented as mean $\pm$ SEM; *, $p < .05$ compared to control siRNA). **(E, F):** Level of Wnt11 mRNA **(E)** and protein **(F)** after β-catenin siRNA transfection (cells cultured in Adipo media [adipogenic induction media] following transfection; Wnt11 protein levels normalized to total protein; data are represented as mean $\pm$ SEM; *, $p < .05$ compared to Adipo + control siRNA). **(G–I):** Silencing of Wnt11 in β-catenin siRNA transfected cells (simultaneous silencing) effectively knocks down mRNA **(G)** and protein levels **(H, I)** of both Wnt11 and β-catenin (β-catenin and Wnt11 protein levels normalized to total protein; data are represented as mean $\pm$ SEM; *, $p < .05$ compared to control siRNA). **(J):** Extent of adipogenesis following Wnt11 knockdown in β-catenin siRNA transfected cells (data are represented as mean $\pm$ SEM; *, $p < .05$ compared to β-catenin siRNA only).

alterations in cells with vasculogenic ability [16, 17, 25]. These subsets may comprise MPCs as well as cells which give rise to endothelial progenitor cells as we have shown previously [16, 18, 25, 26]. The qualitative analysis demonstrated a lower number of CD133+CD45− cells in the diabetic bone marrow, alongside an increase in adipocytes that was not evident in our control samples (Fig. 5A, 5B). Increased bone marrow adiposity has been shown in human diabetes [27] and in animal models of diabetes [28, 29]. Our findings nicely highlight the potential functional consequence of increased adiposity. The reduction in CD133-expressing cells may be due to depletion (i.e., MPCs differentiating into adipocytes thereby reducing the number of CD133-expressing cells) or a nonpermissive change in the stem cell microenvironment.

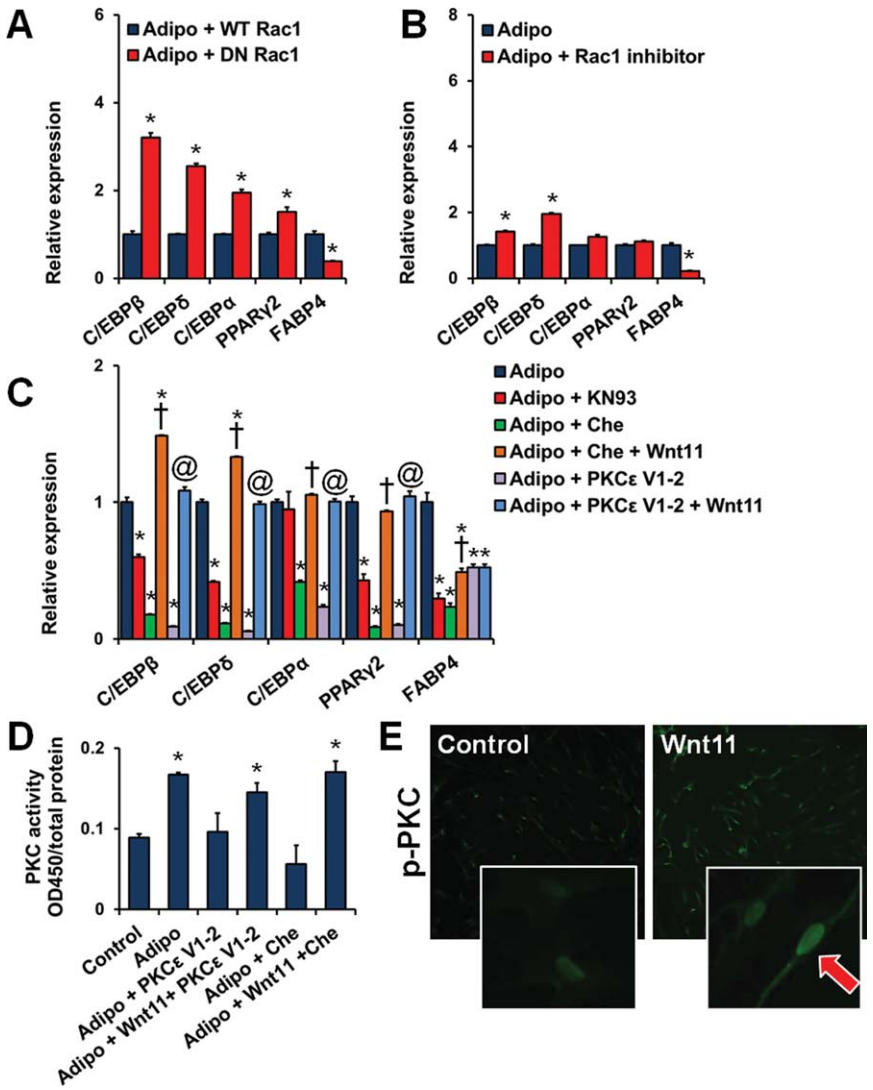

Figure 4. Wnt11 stimulates PKC to increase adipogenesis. **(A):** Extent of adipogenesis after transfection of mesenchymal progenitor cells (MPCs) with DN and WT Rac1 (data are represented as mean ± SEM; *, $p < .05$ compared to WT Rac1). **(B):** mRNA of adipogenesis-specific transcription factors and FABP4 after treatment with Rac1 antagonist (data are represented as mean ± SEM; *, $p < .05$ compared to Adipo). **(C):** Extent of adipogenesis following treatment with calmodulin-dependent protein kinase (CamKII) inhibitor KN93, general PKC inhibitor Che, PKCε-specific inhibitor peptide PKCε V1–2, or PKC inhibitors in the presence of recombinant Wnt11 (data are represented as mean ± SEM; *, $p < .05$ compared to Adipo; †, $p < .05$ compared to Adipo + Che; @, $p < .05$ compared to Adipo + PKCε V1–2). **(D):** PKC activity level following exposure to Adipo, PKC inhibitors, and PKC inhibitors in the presence of Wnt11 (data are represented as mean ± SEM; *, $p < .05$ compared to control). **(E):** Staining of phospho-PKC (p-PKC) in MPCs after treatment with Wnt11 (50 ng/ml) for 24 hours in normal media (Green = phospho-PKC; ×20 magnification; inset at ×40; red arrow showing specific nuclear localization). Abbreviations: DN, dominant negative; PKC, pan-protein kinase C; WT, wild type.

HG Modulates Angiopoietin-2

We looked at various factors that may be responsible for maintaining stem cells in a quiescent/undifferentiated state, including nitric oxide (NO), stromal cell-derived factor-1 (SDF-1), and angiopoietin-1 (Ang1) and -2 (Ang2) (reviewed in [30]). Although we found no changes in NO, CXCL12 (SDF-1), or CXCR4 (SDF-1 receptor) (data not shown), we did note the dramatic elevation of Ang2 mRNA expression in diabetic bone marrow samples (Fig. 5C). Because Ang1 and Ang2 bind to the same Tie2 receptor but antagonize each other's actions [31, 32], we examined the ratio of Ang1 to Ang2 in our samples and show a significant reduction in diabetic bone marrow (Fig. 5D), indicating a possible role for Ang2 in altering homeostasis and possibly disrupting the stem cell niche. Interestingly, diabetes is associated with vascular remodeling in the marrow [8] as well as inflammation [33], both reminiscent of Ang2 actions. We also noted an increase in Tie2 mRNA in diabetic bone marrow (Fig. 5E), indicating a potential upregulation of the antagonistic Ang-Tie signaling system in a HG setting. Because of the predominant number of adipocytes in the marrow samples, we reasoned that adipocytes are the source of Ang2. In support of this concept, we induced the differentiation of MPCs into adipocytes in the presence or absence of HG. As expected, cells treated with HG exhibited significantly higher Ang2 mRNA levels (Fig. 5F) and Ang2 protein in culture media (Fig. 5G).

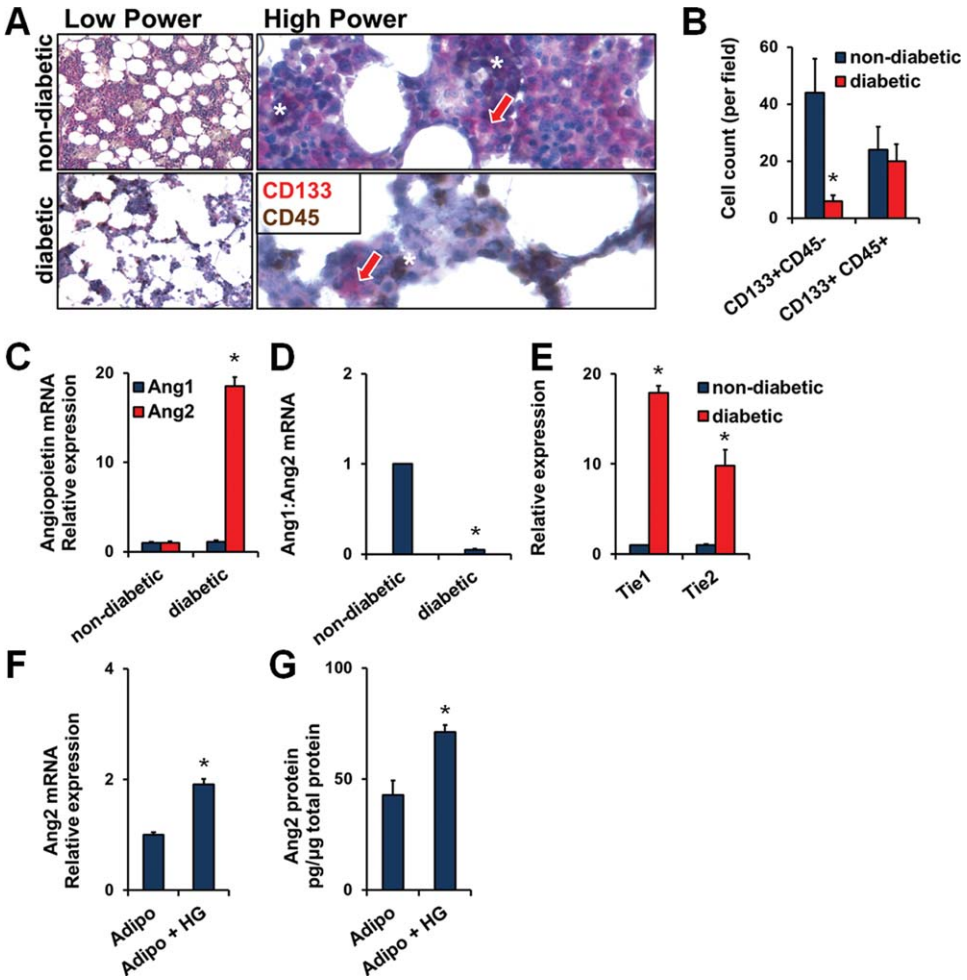

Figure 5. HG modulates angiopoietin-2 in diabetic bone marrow. **(A):** Staining of vasculogenic stem cells (CD133+CD45−; red arrow) and hematopoietic stem cells (HSCs; CD133+CD45+; asterisk) in control and type 2 diabetic bone marrow samples. **(B):** Quantification of stem cells in human marrow samples (data are represented as mean ± SEM; *, $p < 0.05$ compared to nondiabetic). **(C):** mRNA levels of Ang1 and Ang2 in diabetic and nondiabetic marrow samples (data are represented as mean ± SEM; *, $p < 0.05$ compared to nondiabetic). **(D):** Normalized ratio of Ang1/Ang2 in diabetic marrow samples (*, $p > 0.05$ compared to nondiabetic). **(E):** mRNA levels of Tie1 and Tie2 (angiopoietin receptors) in diabetic bone marrow (data are represented as mean ± SEM; *, $p < 0.05$ compared to nondiabetic). **(F):** mRNA expression of Ang2 after differentiation of MPCs to the adipocyte lineage in the presence or absence of HG (data are represented as mean ± SEM; *, $p < 0.05$ as compared to Adipo without HG). **(G):** Ang2 protein levels in culture media after differentiation of MPCs in the presence of HG (48-hour media collected at day 7; Ang2 normalized to total protein levels; data are represented as mean ± SEM; *, $p < 0.05$ compared to Adipo). Abbreviation: HG, high glucose.

Since type 2 diabetes is associated with increased insulin levels and dyslipidemia in addition to hyperglycemia, we used a type 1 diabetic rat model to corroborate the HG effect independent of hyperinsulinemia and dyslipidemia. We obtained femur bone tissues from 2-month-old diabetic and control rats (Fig. 6A) and stained for Ang2. A very distinct staining pattern was noted in the diabetic samples, with Ang2 being localized to the marrow adipocytes specifically (Fig. 6B). This staining pattern supports the deregulation of Ang1/2 upon MPC differentiation, and indicates that the adipocytes themselves are upregulating these proteins in response to HG. In addition, diabetic marrow displayed more immunoreactivity for Ang2 than control marrow highlighting the effect of hyperglycemia. Lastly, we stained for Wnt11 to confirm a seminal role for this protein in HG-mediated adipogenesis. We noted Wnt11 staining of stem/progenitor cells clustered around the adipocytes (Fig. 6C). This localization pattern points to a cell autogenous role of Wnt11 in initiating differentiation.

Discussion

This study establishes the molecular mechanisms behind the skewing of MPC differentiation potential by HG levels and examines, in a broader sense, how this may participate in diabetic bone pathology. The salient findings of our study include: (a) HG "primes" MPCs, reprogramming autocrine Wnt signaling, (b) there is a switch from canonical to noncanonical Wnt signaling in adipogenesis, and (c) the noncanonical Wnt11/PKC pathway is responsible for the skewing of lineage potential that is seen in MPCs in HG (Fig. 7).

Much of what we know about the process of adipogenesis comes from studies in rodent cell lines (e.g., 3T3-L1 mouse embryo-derived "preadipocytes") and rodent multipotential cells. The process involves two phases: the initial commitment phase and the later terminal differentiation phase [34]. Wnt signaling has been linked to the initial commitment phase where canonical and noncanonical ligands have been shown

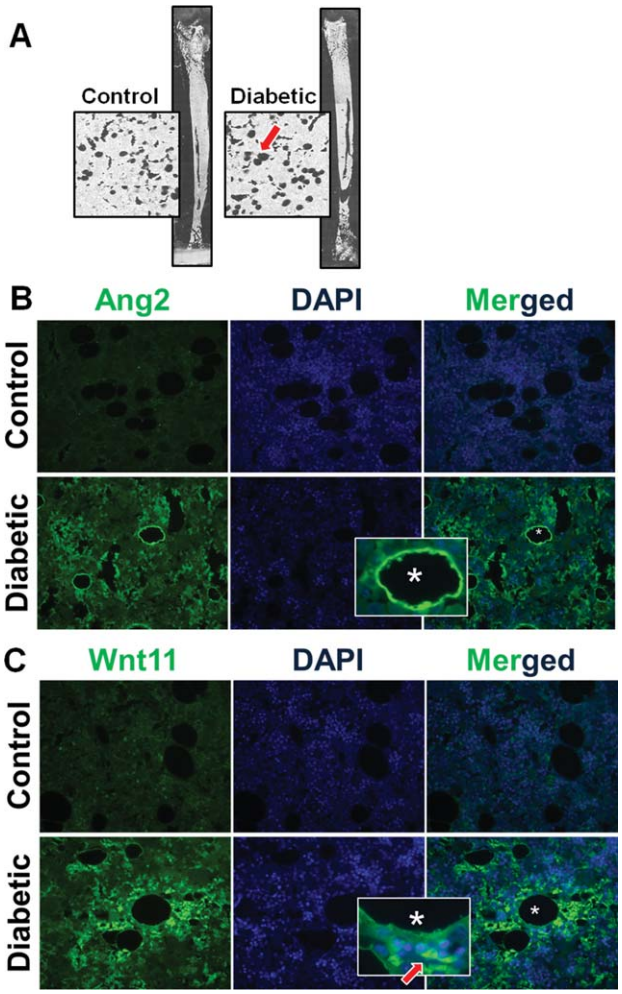

Figure 6. Bone marrow of diabetic rats show increased Wnt11 and Ang2. **(A):** Phase-contrast map of control and type1 diabetic rat bone samples (red arrow highlighting adipocytes). **(B):** Ang2 immunostaining in control and type 1 diabetic rat bone marrow tissues (Green = Ang2; blue = DAPI; asterisk shows a representative Ang2 immunoreactive adipocyte; immunostaining at ×40 magnification). **(C):** Wnt11 immunostaining in control and type 1 diabetic rat bone marrow. Red arrow signifies cells positive for Wnt11 around the adipocytes (Green = Wnt11; blue = DAPI; immunostaining at ×40 magnification). Abbreviation: DAPI, 4′,6-diamidino-2-phenylindole.

to regulate adipogenesis-specific transcription factors. Addition of Wnt10b inhibits PPARγ and reduces adipogenesis whereas knockout of low density lipoprotein receptor-related protein 6 enhances adipogenesis [35, 36]. Interestingly, this signaling pathway tightly regulates osteogenesis as well. Addition of the same Wnt10b has been shown to enhance osteogenesis in rodent bone marrow-derived ST2 (stromal cell line) cells [37]. Reports of both positive [38] and negative [39, 40] regulation of adipogenesis by noncanonical Wnts are also ample. Early studies indicated a positive role for noncanonical Wnts in the regulation of bone mass [39, 41, 42]. However, a more recent study has convincingly demonstrated enhanced bone resorption by noncanonical signaling [43].

We have provided experimental evidence that β-catenin protein is required for adipogenesis in human bone marrow-derived MPCs. This role of β-catenin seems to be independent

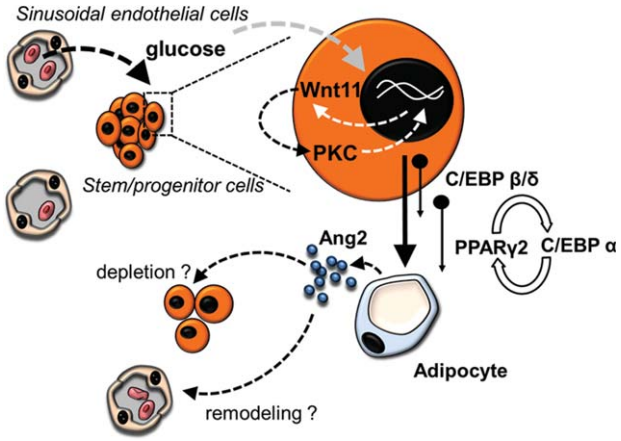

Figure 7. Schematic showing summary of major findings. Our working model based on the findings of this study suggests that high levels of glucose in diabetes cause increased expression of Wnt11 in mesenchymal progenitor cells (MPCs). Wnt11 then primes MPCs to differentiate into adipocytes through activation of PKC. Imbalance between adipocytes and osteoblasts may alter Ang/tie signaling within the bone marrow stem cell niche although decreased Ang1/Ang2 ratio. Ang2 may also be involved in direct depletion of stem cells and vascular remodeling in the bone marrow.

of transcription-mediated mechanisms. Interestingly, complete suppression of β-catenin induced an unexpected increase in adipogenesis and represented a switch from canonical to noncanonical Wnt signaling, evidenced by the dramatic elevation of Wnt11. This enhanced adipogenesis was abolished when Wnt11 was silenced. Therefore, our study provides evidence for an important role of noncanonical Wnt signaling as a major player in adipogenesis. We also set out to examine the dual noncanonical pathways in order to establish a comprehensive understanding of Wnt signaling in the process of adipogenesis. While the Wnt/PCP pathway seems to inhibit adipogenesis, the Wnt/PKC pathway positively regulated this process. With the use of both a general PKC and PKCε-specific inhibitor, we were able to suppress adipogenesis. Further studies must be done in order to elucidate whether essential adipogenic transcription factors PPARγ2 and c/EBPs are a direct target of PKC.

Conclusion

Since MPCs are an important cellular constituent of bone marrow and are thought to give rise to the mesenchymal lineage cells including osteoblasts, chondrocytes, and adipocytes, chronic hyperglycemia in diabetes may be altering the cellular makeup of the bone marrow. Bone loss and increased marrow adiposity have become hallmarks of the diabetic bone phenotype [1, 2], although not much is known about the mechanisms behind these changes. Based on our findings, we can postulate that hyperglycemia induces Wnt11 in marrow MPCs leading to increased adipogenesis and impaired osteogenesis. Enhanced adipogenesis is associated with elevated Ang2 expression. We know that Ang1-Tie2 signaling is involved in the long-term repopulation of bone marrow HSCs, crucial for the maintenance of the stem cell niche [44]. Elevated Ang2 in diabetes may disrupt Ang1-Tie2 signaling reducing stem/progenitor cells in diabetic bone marrow. Elevated Ang2 may also play a role in microvascular remodeling and inflammation in the bone marrow of diabetic patients. These observations

certainly warrant further studies on the functional significance of marrow Ang2 in diabetes.

Acknowledgments

We would like to acknowledge support from the Canadian Diabetes Association (OG-3–13-4034-ZK and OG-3–09-2874-ZK to ZAK), National Institutes of Health (EY007739, EY012601, DK090730 to MBG), and the Lawson Health Research Institute (Z.A.K.). Z.A.K. is a recipient of a New Investigator Award from the Heart and Stroke Foundation of Canada (Great-West Life and London Life New Investigator Award). We also thank Amy S. Porter, Michigan State University, for preparing tissues for immunostaining.

Author Contributions

E.C.K.: designed and carried out most of the experiments, interpreted the data, and drafted the manuscript; J.M.D.: maintained the diabetic animals and performed clinical monitoring; M.B.G.: provided clinical expertise, supervised animal experiments, and edited the manuscript; Z.A.K.: conceived the project, interpreted the data, edited, and finalized the manuscript.

Disclosure of Potential Conflicts of Interest

The authors indicate no potential conflicts of interest.

References

1 Botolin S, Faugere MC, Malluche H et al. Increased bone adiposity and peroxisomal proliferator-activated receptor-gamma2 expression in type I diabetic mice. Endocrinology 2005;146:3622–3631.

2 Botolin S, McCabe LR. Bone loss and increased bone adiposity in spontaneous and pharmacologically induced diabetic mice. Endocrinology 2007;148:198–205.

3 Bouillon R. Diabetic bone disease. Calcif Tissue Int 1991;49:155–160.

4 Hough S, Avioli LV, Bergfeld MA et al. Correction of abnormal bone and mineral metabolism in chronic streptozotocin-induced diabetes mellitus in the rat by insulin therapy. Endocrinology 1981;108:2228–2234.

5 Glajchen N, Epstein S, Ismail F et al. Bone mineral metabolism in experimental diabetes mellitus: Osteocalcin as a measure of bone remodeling. Endocrinology 1988;123:290–295.

6 Schwartz AV, Sellmeyer DE, Ensrud KE et al. Older women with diabetes have an increased risk of fracture: A prospective study. J Clin Endocrinol Metab 2001;86:32–38.

7 de L, II, van der Klift M, de Laet CE et al. Bone mineral density and fracture risk in type-2 diabetes mellitus: The Rotterdam Study. Osteoporos Int 2005;16:1713–1720.

8 Oikawa A, Siragusa M, Quaini F et al. Diabetes mellitus induces bone marrow microangiopathy. Arterioscler Thromb Vasc Biol 2010;30:498–508.

9 Spinetti G, Cordella D, Fortunato O et al. Global remodeling of the vascular stem cell niche in bone marrow of diabetic patients: Implication of the microRNA-155/FOXO3a signaling pathway. Circ Res 2013;112:510–522.

10 Keats E, Khan ZA. Unique responses of stem cell-derived vascular endothelial and mesenchymal cells to high levels of glucose. PLoS One 2012;7:e38752.

11 Kestler HA, Kuhl M. From individual Wnt pathways towards a Wnt signalling network. Philos Trans R Soc Lond B Biol Sci 2008;363:1333–1347.

12 Ross SE, Hemati N, Longo KA et al. Inhibition of adipogenesis by Wnt signaling. Science 2000;289:950–953.

13 Chocarro-Calvo A, Garcia-Martinez JM, Ardila-Gonzalez S et al. Glucose-induced beta-catenin acetylation enhances Wnt signaling in cancer. Mol Cell 2013;49:474–486.

14 Anagnostou SH, Shepherd PR. Glucose induces an autocrine activation of the Wnt/beta-catenin pathway in macrophage cell lines. Biochem J 2008;416:211–218.

15 Lin CL, Wang JY, Huang YT et al. Wnt/beta-catenin signaling modulates survival of high glucose-stressed mesangial cells. J Am Soc Nephrol 2006;17:2812–2820.

16 Khan ZA, Melero-Martin JM, Wu X et al. Endothelial progenitor cells from infantile hemangioma and umbilical cord blood display unique cellular responses to endostatin. Blood 2006;108:915–921.

17 Khan ZA, Boscolo E, Picard A et al. Multipotential stem cells recapitulate human infantile hemangioma in immunodeficient mice. J Clin Invest 2008;118:2592–2599.

18 Keats EC, Khan ZA. Vascular stem cells in diabetic complications: Evidence for a role in the pathogenesis and the therapeutic promise. Cardiovasc Diabetol 2012;11:37.

19 Tanaka S, Terada K, Nohno T. Canonical Wnt signaling is involved in switching from cell proliferation to myogenic differentiation of mouse myoblast cells. J Mol Signal 2011;6:12.

20 Chen B, Dodge ME, Tang W et al. Small molecule-mediated disruption of Wnt-dependent signaling in tissue regeneration and cancer. Nat Chem Biol 2009;5:100–107.

21 Schlessinger K, Hall A, Tolwinski N. Wnt signaling pathways meet Rho GTPases. Genes Dev 2009;23:265–277.

22 Koh CG. Rho GTPases and their regulators in neuronal functions and development. Neurosignals 2006;15:228–237.

23 Wojciak-Stothard B, Ridley AJ. Rho GTPases and the regulation of endothelial permeability. Vascul Pharmacol 2002;39:187–199.

24 Webb PR, Doyle C, Anderson NG. Protein kinase C-epsilon promotes adipogenic commitment and is essential for terminal differentiation of 3T3-F442A preadipocytes. Cell Mol Life Sci 2003;60:1504–1512.

25 Melero-Martin JM, Khan ZA, Picard A et al. In vivo vasculogenic potential of human blood-derived endothelial progenitor cells. Blood 2007;109:4761–4768.

26 Melero-Martin JM, De Obaldia ME, Kang SY et al. Engineering robust and functional vascular networks in vivo with human adult and cord blood-derived progenitor cells. Circ Res 2008;103:194–202.

27 Slade JM, Coe LM, Meyer RA et al. Human bone marrow adiposity is linked with serum lipid levels not T1-diabetes. J Diabetes Complications 2012;26:1–9.

28 Motyl K, McCabe LR. Streptozotocin, type I diabetes severity and bone. Biol Proced Online 2009;11:296–315.

29 Botolin S, McCabe LR. Inhibition of PPARgamma prevents type I diabetic bone marrow adiposity but not bone loss. J Cell Physiol 2006;209:967–976.

30 Frenette PS, Pinho S, Lucas D et al. Mesenchymal stem cell: Keystone of the hematopoietic stem cell niche and a stepping-stone for regenerative medicine. Annu Rev Immunol 2013;31:285–316.

31 Maisonpierre PC, Suri C, Jones PF et al. Angiopoietin-2, a natural antagonist for Tie2 that disrupts in vivo angiogenesis. Science 1997;277:55–60.

32 Gomei Y, Nakamura Y, Yoshihara H et al. Functional differences between two Tie2 ligands, angiopoietin-1 and −2, in regulation of adult bone marrow hematopoietic stem cells. Exp Hematol 2010;38:82–89.

33 Yellowlees Douglas J, Bhatwadekar AD, Li Calzi S et al. Bone marrow-CNS connections: Implications in the pathogenesis of diabetic retinopathy. Prog Retin Eye Res 2012;31:481–494.

34 Cristancho AG, Lazar MA. Forming functional fat: A growing understanding of adipocyte differentiation. Nat Rev Mol Cell Biol 2011;12:722–734.

35 Kawai M, Mushiake S, Bessho K et al. Wnt/Lrp/beta-catenin signaling suppresses adipogenesis by inhibiting mutual activation of PPARgamma and C/EBPalpha. Biochem Biophys Res Commun 2007;363:276–282.

36 Longo KA, Wright WS, Kang S et al. Wnt10b inhibits development of white and brown adipose tissues. J Biol Chem 2004;279:35503–35509.

37 Kang S, Bennett CN, Gerin I et al. Wnt signaling stimulates osteoblastogenesis of mesenchymal precursors by suppressing CCAAT/enhancer-binding protein alpha and peroxisome proliferator-activated receptor gamma. J Biol Chem 2007;282:14515–14524.

38 Kanazawa A, Tsukada S, Kamiyama M et al. Wnt5b partially inhibits canonical Wnt/beta-catenin signaling pathway and promotes adipogenesis in 3T3-L1 preadipocytes.

Biochem Biophys Res Commun 2005;330: 505–510.

39 Takada I, Mihara M, Suzawa M et al. A histone lysine methyltransferase activated by non-canonical Wnt signalling suppresses PPAR-gamma transactivation. Nat Cell Biol 2007;9:1273–1285.

40 Wakabayashi K, Okamura M, Tsutsumi S et al. The peroxisome proliferator-activated receptor gamma/retinoid X receptor alpha heterodimer targets the histone modification enzyme PR-Set7/Setd8 gene and regulates adipogenesis through a positive feedback loop. Mol Cell Biol 2009;29: 3544–3555.

41 Tu X, Joeng KS, Nakayama KI et al. Noncanonical Wnt signaling through G protein-linked PKCdelta activation promotes bone formation. Dev Cell 2007;12:113–127.

42 Chang J, Sonoyama W, Wang Z et al. Noncanonical Wnt-4 signaling enhances bone regeneration of mesenchymal stem cells in craniofacial defects through activation of p38 MAPK. J Biol Chem 2007;282:30938–30948.

43 Maeda K, Kobayashi Y, Udagawa N et al. Wnt5a-Ror2 signaling between osteoblast-lineage cells and osteoclast precursors enhances osteoclastogenesis. Nat Med 2012; 18:405–412.

44 Arai F, Hirao A, Ohmura M et al. Tie2/angiopoietin-1 signaling regulates hematopoietic stem cell quiescence in the bone marrow niche. Cell 2004;118:149–161.

